Development of Conducting Polyaniline/Poly(lactic acid) Nanofibers by Electrospinning

Paulo H. S. Picciani,[1] Eliton S. Medeiros,[2,3] Zhongli Pan,[4,5] William J. Orts,[3] Luiz H. C. Mattoso,[2,3] Bluma G. Soares[1]

[1]*Instituto de Macromoléculas, Centro de Tecnologia, Universidade Federal do Rio de Janeiro, Bloco J, Ilha do Fundão, P.O. Box 68525, Rio de Janeiro RJ, Brazil 21945-970*
[2]*Laboratório Nacional de Nanotecnologia Aplicada ao Agronegócio, Embrapa Instrumentação Agropecuária, Rua XV de Novembro 1452, São Carlos SP, Brazil 13560-970*
[3]*Bioproducts Chemistry and Engineering Unit, Western Regional Research Center, Agricultural Research Services, U.S. Department of Agriculture, Albany, CA 94710*
[4]*Processed Foods Research Unit, Western Regional Research Center, Agricultural Research Services, U.S. Department of Agriculture, Albany, CA 94710*
[5]*Department of Biological and Agricultural Engineering, University of California at Davis, One Shields Avenue, Davis, CA 95616*

Received 21 July 2008; accepted 15 October 2008
DOI 10.1002/app.29447
Published online 13 January 2009 in Wiley InterScience (www.interscience.wiley.com).

ABSTRACT: Ultrafine fibers consisting of blends of polyaniline doped with *p*-toluene sulfonic acid and poly(L-lactic acid) were prepared by electrospinning. The presence of polyaniline resulted in fibers with diameters as thin as 100–200 nm and a significant reduction of bead formation. These fibers were visually homogeneous, and this indicated good interactions between the components of the polyaniline/poly(L-lactic acid) blend. The high interaction between the components and the rapid evaporation of the solvent during electrospinning resulted in nanofibers with a lower degree of crystallinity in comparison with cast films. The electrical conductivity of the electrospun fiber mats was lower than that of blend films produced by casting, probably because of the lower degree of crystallinity of the polyaniline dispersion and the high porosity of the nonwoven mat. This novel system opens up new and interesting opportunities for applications in biomedical devices, biodegradable materials, and sensors, among other things. © 2009 Wiley Periodicals, Inc. J Appl Polym Sci 112: 744–753, 2009

Key words: conducting polymers; electron microscopy; fibers; nanocomposites

INTRODUCTION

Nanofibers of conducting polymers and their blends with conventional insulating polymers have received great attention over the last decade because of their unique and useful properties,[1] which are important for several potential applications such as electronic devices in optics and electronic and biomedical materials,[2–4] protective clothing,[5] filtration media,[6] charge storage devices,[7,8] and sensors and actuators.[9–11] Among conducting polymers, polyaniline (PAni) is considered one of the most technologically promising because of its simple and reversible doping/redoping chemistry, its high environmental stability, and the low cost of the monomer (aniline). PAni-based nanostructured materials, including nanofibers, nanotubes, and nanowires, have been produced in different ways.[12] Among these, the electrostatic spinning process has emerged as an efficient and promising technique for the preparation of fibers with diameters in the submicrometer to micrometer range because of its simplicity and its ability to scale up into a continuous process.[13,14]

In this process, a high-voltage electric field is applied between a polymer solution or melt (contained in a glass syringe with a capillary dip) and a collector screen. When the applied voltage is balanced with the surface tension of the polymer solution, a Taylor cone is initiated;[15–17] that is, the suspended solution meniscus turns into a cone with a semivertical angle of 49.3°. Beyond this critical value, the electrostatic forces generated by the charge carriers (which move toward the surface of the polymer solution) overcome the surface tension

Correspondence to: L. H. C. Mattoso (mattoso@cnpdia.embrapa.br) or B. G. Soares (bluma@ima.ufrj.br).

Contract grant sponsor: Conselho Nacional de Desenvolvimento Científico e Tecnológico; contract grant number: 210237/2006-6.
Contract grant sponsor: Coordenação de Aperfeiçoamento de Pessoal de Nivel Superior.
Contract grant sponsor: Fundação de Amparo à Pesquisa do Estado do Rio de Janeiro.
Contract grant sponsor: Embrapa/U.S. Department of Agriculture Labex program.

of the deformed drop of the suspended polymer solution, initiating the formation of a fiber jet from the cone tip, which is collected on the collector screen.

During the electrospinning of fibers, the electrically charged jet undergoes tension instabilities; this results in bending and stretching, which are accompanied by the reduction of the jet diameter and rapid solvent evaporation. The dry fibers are collected on the surface of the oppositely charged collector screen as a fiber mat.[18] One of the great advantages of this process is the ability to produce fibers as a nonwoven mat with a high surface area and high porosity. These characteristics are of paramount importance for the development of several electronic devices, as mentioned previously.

Electrospinning technology has been successfully employed to prepare PAni-based conducting nanofibers from a solution of pure PAni.[1,19] Nevertheless, the use of a solution blend of PAni with other conventional polymers is somewhat preferred because the conventional polymer may assist with the formation of PAni fiber and also act as a support material for the nanofiber. Some polymers have been employed for this purpose, including poly(ethylene oxide),[20] nylon-6,[21] and polystyrene.[10,22] To the best of our knowledge, there is no report in the accessible literature regarding the use of poly(L-lactic acid) (PLA) as the support polymeric matrix for the preparation of PAni-based conducting nanofibers. PLA and its copolymers are biodegradable and biocompatible, present good thermoplastic processability, and have potential applications as commodity plastics to be used in agricultural products and disposable materials.[23] Because of its biocompatibility, PLA is often used as the base material for implant devices, such as suture fibers and scaffolds for tissue engineering.[24] Recently, it has been employed in nanofiber preparation with the electrospinning technique.[25–27] Therefore, PLA is a promising candidate for the preparation of conducting nanofibers in combination with PAni for sensors and other applications.

The aim of this work was to prepare conducting nanofibers from PAni/PLA blends with a special focus on the influence of some operational parameters, such as the polymer concentration, applied voltage, and flow rate, on the morphology of electrospun fibers. The degree of crystallinity and conductivity of the electrospun PAni/PLA nanofibers were also evaluated and compared to those observed for cast films.

EXPERIMENTAL

Materials

PLA (polylactide resin 4042D) with a molecular weight of 66,000 g/mol was acquired from NatureWorks LLC (Minnetonka, MN). Aniline (analytical-grade; Sigma–Aldrich) [St. Louis, MO], 1,1,1,3,3,3-hexafluoro-2-propanol (HFP; Sigma–Aldrich) [St. Louis, MO], ammonium peroxydisulfate (Mallinckrodt, Inc.), a 1 mol/L hydrochloric acid (HCl) solution (Sigma–Aldrich) [St. Louis, MO], and *p*-toluene sulfonic acid (TSA; analytical-grade; Sigma–Aldrich [St. Louis, MO]) were used without further purification.

PAni synthesis

PAni in the emeraldine salt (ES) form was chemically synthesized according to the method described by MacDiarmid and Epstein.[28] In a typical procedure, 10 mL of aniline was dissolved in 150 mL of a 1 mol/L HCl solution at 0°C. The oxidant ammonium peroxydisulfate (0.5760 g), which had been previously dissolved in 100 mL of an HCl solution (1 mol/L), was cooled and dropped into the reaction medium over 20 min. After 2 h, the resultant dark-green solid was filtered and washed several times with an HCl solution. The emeraldine base (EB) form of PAni was obtained by the treatment of ES with a 0.1*M* NH_4OH solution for 24 h. The dark-blue solid was filtered, washed with the NH_4OH solution, and dried *in vacuo* until a constant weight was obtained.

Solution preparation

EB PAni (0.003 g, 2.76×10^{-5} mol) and 0.003 g (5.81×10^{-5} mol) of TSA were dissolved in a proper amount of HFP under magnetic stirring for 2 h to obtain 0.2, 0.4, and 0.6 wt % solutions of polyaniline doped with *p*-toluene sulfonic acid (PAni·TSA). The same procedure was used to prepare 10 and 12 wt % solutions of PLA in HFP. Then, the solutions were filtered, and equal volumes of PAni·TSA and PLA solutions were mixed in the eight different combinations shown in Table I.

Electrospinning setup

The electrospinning apparatus, shown in Figure 1, was equipped with a high-voltage power supply (series FC, Glassman High Voltage, Inc., High Bridge,

TABLE I
Different Combinations of PLA and PAni Solutions Used for Electrospinning

Solution	PLA solution (%)	PAni·TSA solution (%)
1	10	0.0
2	10	0.2
3	10	0.4
4	10	0.6
5	12	0.0
6	12	0.2
7	12	0.4
8	12	0.6

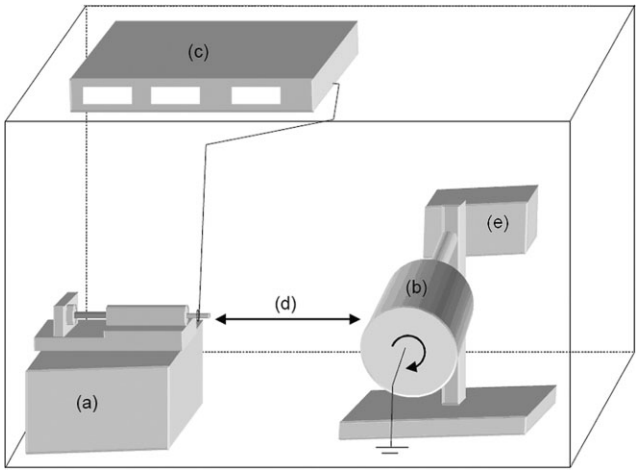

Figure 1 Schematic depiction of the electrospinning setup used for fiber production: (a) injection pump with a hypodermic syringe, (b) grounded collector, (c) high-voltage supply, (d) working distance and (e) motor.

NJ, United States) capable of voltages as high as 99 kV. The polymer solution was added to a 5-mL syringe with a 21G hypodermic needle (i.d. = 0.495 ± 0.001 nm) used as the nozzle. A metallic drum counter electrode with a controlled rotation speed was placed at a working distance of 11.5 cm from the needle. The flow rate of the polymer solution was controlled with a precision pump (KD Scientific, Holliston, MA, United States) to maintain a steady flow from the capillary outlet. The experimental temperature was controlled at 25°C, and the relative humidity was maintained between 40 and 50%. Each solution was injected at two different rates, 4 and 6 μL/min, and the applied voltage was set to 18 or 22 kV. Before each experiment, the collector drum was covered with aluminum foil, which was then removed from the drum after fiber deposition. All the nonwoven fiber mats were dried at room temperature until any solvent residue was completely removed before characterization.

Film casting

To compare the properties of PAni·TSA/PLA blended fibers, freestanding films were prepared with the same solutions listed in Table I. The polymer films were obtained by the drop casting of the solutions onto microscope glass slides at the controlled temperature of 25°C and at a relativity humidity between 40 and 50%. All the films were dried at room temperature until complete solvent removal before characterization.

Morphology

Morphology studies of all nonwoven mats were carried out with scanning electron microscopy (SEM). All the fibers were mounted directly onto aluminum specimen stubs with two-sided adhesive carbon tabs (Pelco, Redding, CA) and coated with gold in a Denton (Moorestown, NJ, New Jersey) Desk II sputter coating unit for approximately 45 s at 20 μA and 75 mTorr. Samples were analyzed in a Hitachi model S-4700 field emission scanning electron microscope (Tokyo, Japan) operating at an accelerating voltage of 2 kV. Digital images were captured at a resolution of 1280 pixels × 960 pixels. Representative micrographs were chosen to illustrate each fiber mat.

X-ray diffraction analysis

Wide-angle X-ray diffraction of the fiber mats, PAni (EB) and PLA powders, and cast films of PAni·TSA/PLA blends was carried out on a Philips X'Pert MPD X-ray diffractometer (Amsterdam, The Netherlands) operated at 45 kV and 40 mA with graphite-filtered Cu $K\alpha_1$ radiation (wavelength = 0.154 nm). The samples were scanned from 1.5 to 40° with a scan rate of 0.1°/s.

Electrical resistivity measurements

Electrical resistivity measurements of the drop-cast films and nonwoven fiber mats were performed according to the ASTM D 257 standard testing method with a Keithley 6517A electrometer (Cleveland, OH, USA) as the source.

RESULTS AND DISCUSSION

Solutions of PLA and its blends with different amounts of PAni·TSA were electrospun at different applied voltages and injection rates. The average diameter values of all the samples were determined on the basis of 50 individual fiber measurements randomly chosen from each SEM image at the same magnification. The average diameter values of the electrospun nanofibers are summarized in Table II as functions of the polymer concentrations (PLA and PAni·TSA), applied voltage, and flow rate.

Mats with the smallest average fiber diameters are presented in bold. A significant decrease in the fiber diameter was observed for PAni·TSA/PLA blends, and this strongly depended on the PAni·TSA concentration, as illustrated in Figure 2. Indeed, an interesting quadratic relationship between the average fiber diameter and the PAni content in the solution was observed. This behavior was also found by Gu et al.[29] when they were studying electrospun polyacrylonitrile fibers. The smallest diameters were obtained with PAni·TSA contents between 2 and 4% with respect to PLA. This result may be attributed to an increase in the solution viscosity associated with changes in the dielectric constant and an increase in the charge density. All these features contributed to

TABLE II
Effects of the Electrospinning Parameters on the Average Diameter of the Corresponding Nanofibers Prepared from the PLA and PAni·TSA Blend Solutions

Solution		PLA solution (%)	PAni·TSA solution (%)	Applied voltage (kV)	Rate of injection (μL/m)	Average diameter (nm)	Standard deviation (nm)
1	a	10	0.0	18	4	515.7	240.0
	b			18	6	571.1	237.8
	c			22	4	417.0	160.0
	d			22	6	380.0	129.0
2	a	10	0.2	18	4	253.7	70.0
	b			18	6	274.0	76.5
	c			22	4	262.9	85.5
	d			22	6	154.7	73.3
3	a	10	0.4	18	4	198.4	34.8
	b			18	6	206.8	45.6
	c			22	4	133.8	57.6
	d			22	6	131.8	54.6
4	a	10	0.6	18	4	398.5	91.7
	b			18	6	859.1	270.7
	c			22	4	218.8	51.0
	d			22	6	469.6	173.9
5	a	12	0.0	18	4	400.0	238.7
	b			18	6	520.0	244.4
	c			22	4	525.1	202.0
	d			22	6	622.8	298.1
6	a	12	0.2	18	4	237.09	62.9
	b			18	6	366.91	130.2
	c			22	4	190.36	74.3
	d			22	6	178.36	78.1
7	a	12	0.4	18	4	246.40	84.4
	b			18	6	255.20	69.7
	c			22	4	156.50	85.8
	d			22	6	153.00	63.3
8	a	12	0.6	18	4	263.64	115.2
	b			18	6	246.36	54.4
	c			22	4	462.91	142.7
	d			22	6	560.36	125.9

superior stretching of the polymer jet during the electrospinning process. Beyond a determined point, the increase in the PAni·TSA concentration led to the formation of thicker fibers, probably because of the increase in the chain entanglements, which made the stretching of the charged jet difficult.[30] Because of the conditions used in this work, thin fibers with higher amounts of PAni were obtained when an applied voltage of 18 kV was used. Increasing the applied voltage also gave rise to thinner fibers when the injection rate was lower (4 μL/min), and the initial concentration of the PLA solution in HFP was also lower (10%).

In addition to the fiber diameter, the morphology and the formation of beads were also influenced by the presence of PAni·TSA. Figure 3 presents some SEM micrographs of electrospun fiber mats obtained from PLA (left side) and a PAni·TSA/PLA (0.2 : 10%) solution blend (right side) in HFP at an applied voltage of 18 kV and at different flow rates. The PLA electrospun nanofibers presented high amounts of beads, which could be related to the instability of the jet of the polymer solution, as stated by Yarin.[31] According to the literature, bead formation is related to a combination of a strong applied voltage and a higher injection rate.[32] These conditions affect the formation of the fiber jet because the time spent by the jet from the nozzle to the collector is not long enough to permit the complete evaporation of the solvent. Consequently, the surface tension overcomes the viscoelastic forces, inducing bead formation.[29] The presence of PAni resulted in a drastic decrease in bead formation and also a significant decrease in the fiber diameter. Similar trends have also been observed in fibers obtained at a higher electric field (22 kV; not shown here). These results may be attributed to the increase in the net charge density of the solution in the presence of PAni·TSA, which favors the formation of thin fibers without beads. In addition, as indicated in Table II, the presence of PAni·TSA caused significant changes in the solution viscosity, which also influenced the fiber

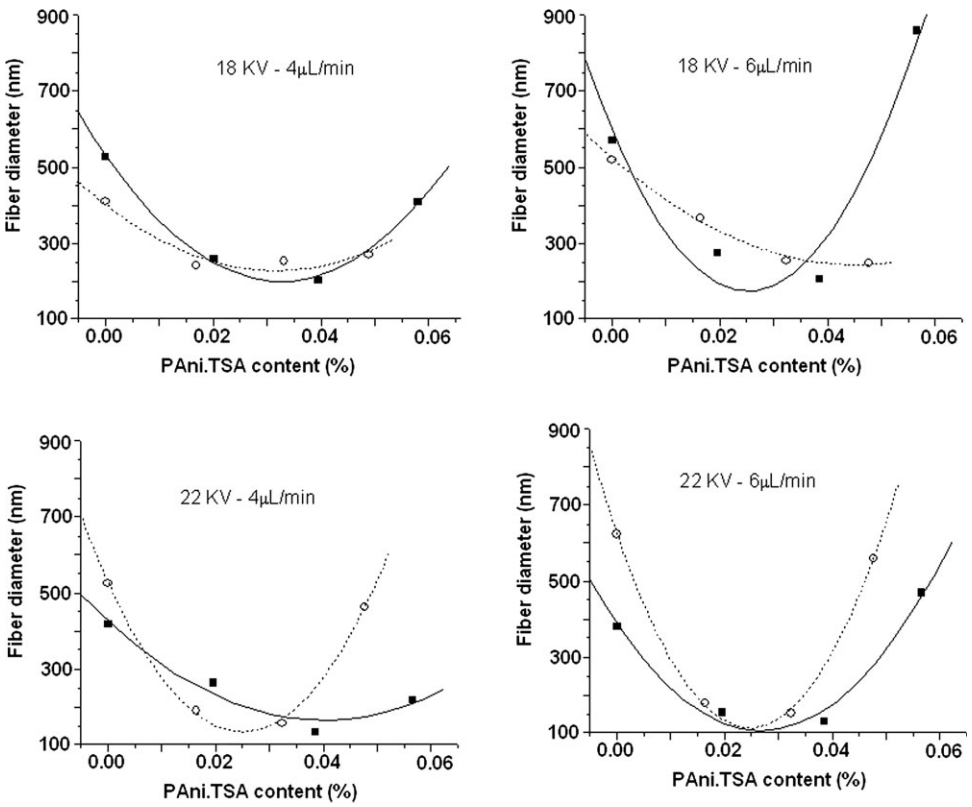

Figure 2 Effect of the PAni·TSA content in the solution blends on the diameter of the electrospun fibers. The concentration of the PLA solution was (■) 10 or (○) 12%.

morphology. The solution containing 0.4% PAni·TSA presented the highest viscosity value and gave rise to fibers with the lowest diameter.

Actually, the following may have happened. The addition of PAni·TSA is almost equivalent to the addition of salts to electrospinning solutions,[33]

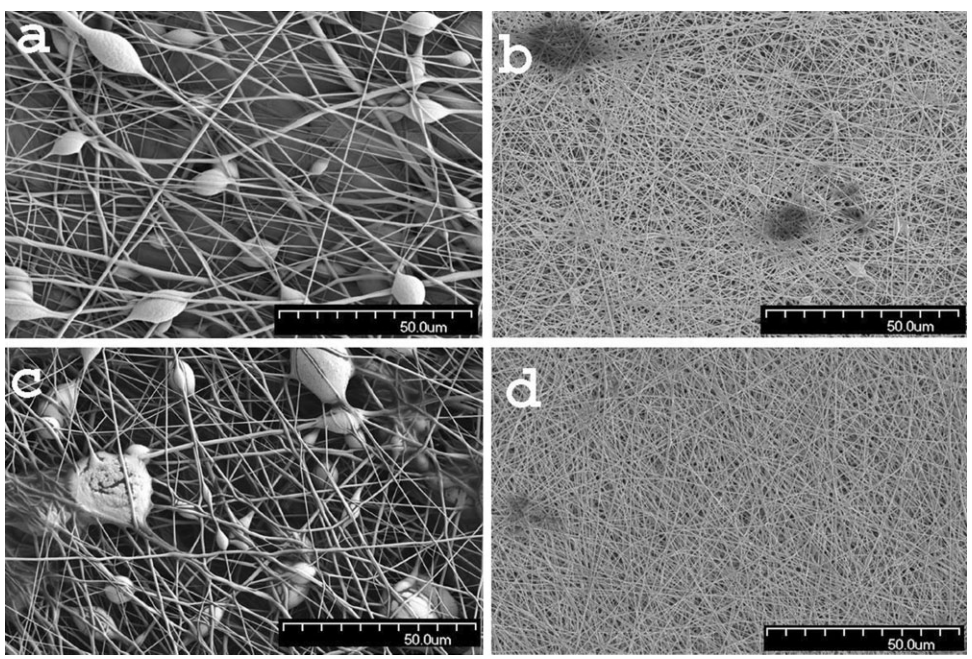

Figure 3 SEM micrographs of electrospun PLA fibers obtained at a flow rate of (a) 4 or (c) 6 μL/min and PAni·TSA/PLA (2 : 100 w/w) blend fibers obtained at a flow rate of (b) 4 or (d) 6 μL/min (applied voltage = 18 kV).

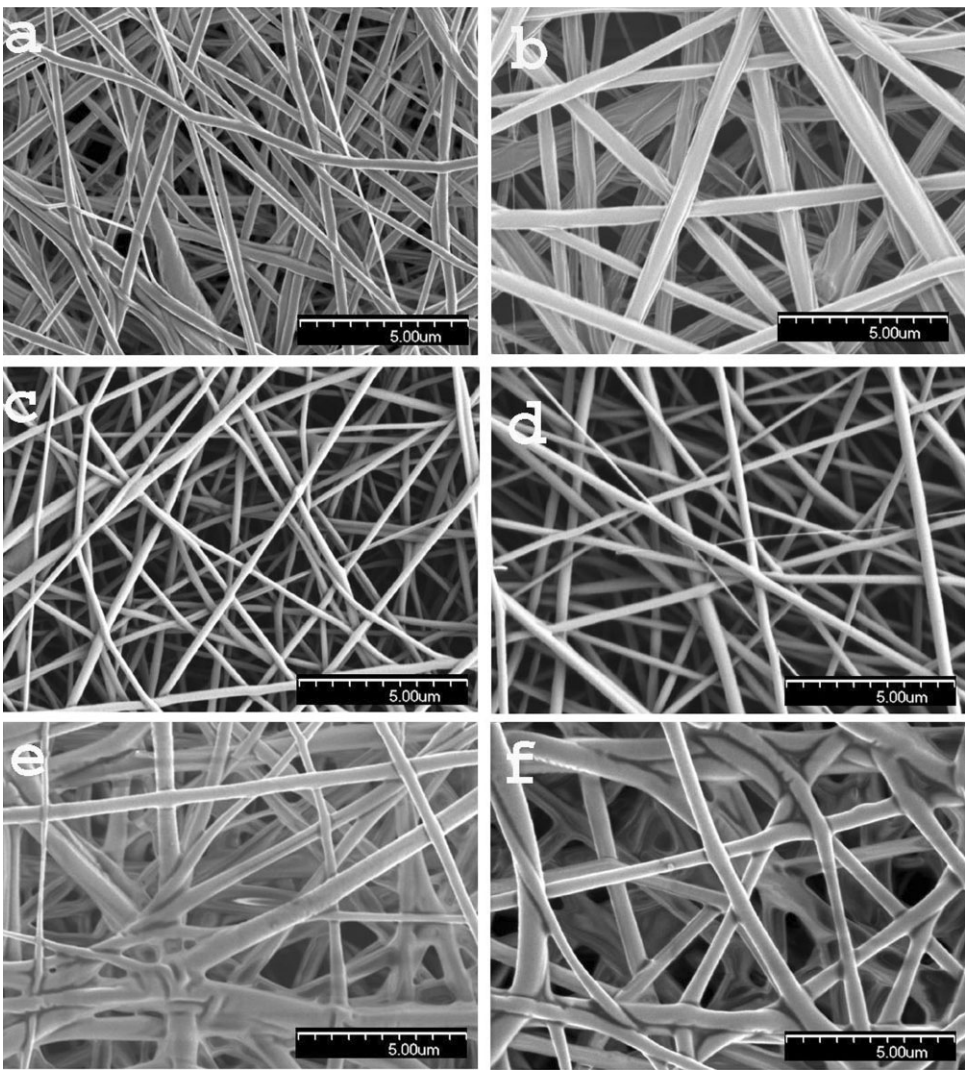

Figure 4 SEM micrographs of electrospun PAni·TSA/PLA blend fibers obtained with initial PAni·TSA/PLA solution concentrations of (a) 0.2/10, (b) 0.2/12, (c) 0.4/10, (d) 0.4/12, (e) 0.6/10, and (f) 0.6/12%.

which affect not only the viscosity but also the ionic conductivity of the solutions. The increase in the ionic conductivity changes the dielectric constant of the medium and makes the movement of two equally charged species on the jet surface easier. The stretching caused by the repulsion of electrostatic charges therefore helps to reduce the fiber diameter.

Figure 4 presents SEM micrographs of PAni·TSA/PLA blend fiber mats as a function of the initial concentration of the PLA solution and the PAni·TSA concentration (taken at a higher magnification). The electrospun nanofibers of all PAni·TSA/PLA blends presented a single phase indicating good interactions between the blend components. Fibers containing higher amounts of PAni·TSA [Fig. 4(e,f)] presented a flat geometry that could be attributed to the higher viscosity of the blends. Even for these fiber mats with higher average diameters, there was no formation of beaded structures. The initial concentration of the PLA solution exerted some influence on the fiber diameter when a lower applied voltage was applied. However, for higher applied voltages and high flow rates, fiber mats presented similar profiles, regardless of the initial concentration of PLA.

All the fiber mats formed very flexible and stable macroscopic structures toward environmental exposure in comparison with the casting films with the same composition. In addition, the fiber mats presented relatively high pH resistance, and PAni·TSA was not dedoped under environmental and water exposition, keeping its green color, which is characteristic of the doped state. Figure 5 shows scanning electron micrographs of the cast films with the same compositions of the electrospun fibers. As one can see, both small and large cracks were present in the cast films, and this indicated that these films were extremely fragile in comparison with the electrospun fiber mats. In addition, evident phase separation in

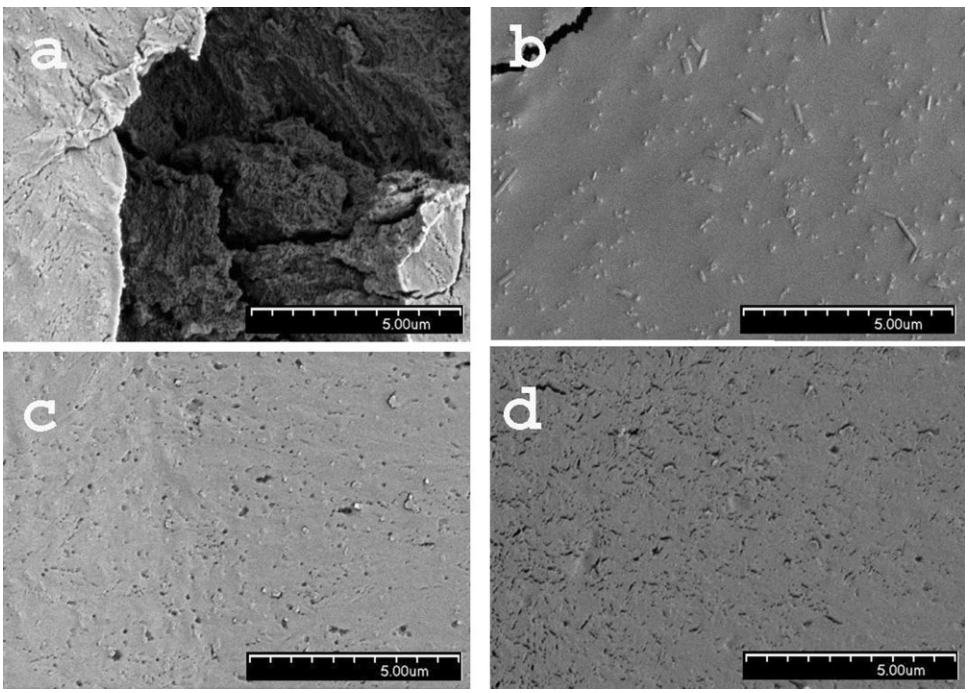

Figure 5 SEM micrographs of cast films of PAni·TSA/PLA in HFP obtained from (a) 0.2/10, (b) 0.6/10, (c) 0.2/12, and (d) 0.6/12% solution blends.

the cast films was observed, in which PAni·TSA complex islands were segregated from the PLA matrix. One of the probable reasons that phase separation did not take place during electrospinning was the very fast solvent evaporation, which took only a fraction of a second, therefore restraining probable phase separation when higher concentrations of PAni·TSA were used in the blends.

The crystallinity degree of PAni·TSA/PLA blends in the form of cast films and electrospun mats was studied with X-ray diffraction. Figure 6 shows the X-ray diffraction patterns of PAni/PLA blends with

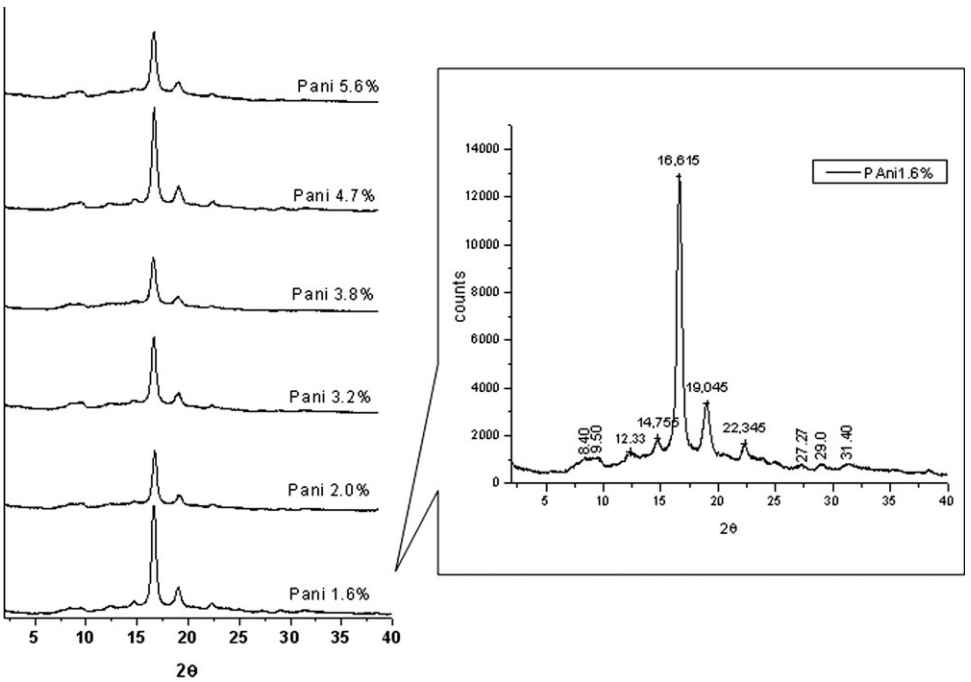

Figure 6 X-ray diffraction of cast films with different PAni·TSA contents.

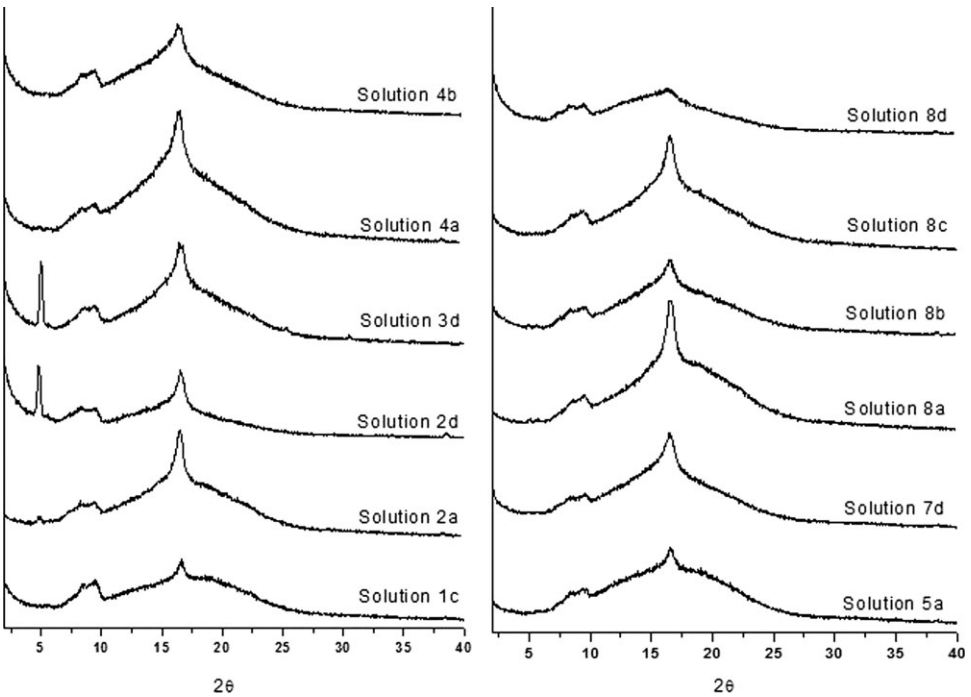

Figure 7 X-ray patterns of 12 selected fiber mats obtained from the solutions listed in Table II.

six different compositions and pure PLA films prepared by casting. All the films presented similar diffraction patterns, with five characteristic peaks at 12.3, 14.8, 16.6, 19, and 22.3°. The very intense peak at 16.6° corresponds to the combined reflections of the (110) and (200) crystalline planes,[34] and the other prominent peak at 19° is related to the (203) plane, confirming the orthorhombic α-crystal structure of the PLA matrix.[34,35] As can be seen in the detailed scattering, the crystalline structure of the PAni·TSA component is characterized by a weak broad peak around 8.40–9.50° and very weak reflections at 27.2, 39, and 31.4° related to doped PAni, as described by Pouget et al.[36]

X-ray diffractograms of some selected fiber mats are shown in Figure 7. These fibers presented the main reflections of the PLA α-crystalline structure and an expressive amorphous halo indicating lower crystallinity values in comparison with the cast films. Moreover, in some fiber samples, small reflections at 25 and 30° revealed the coexistence of the α- and β-crystal structures of PLA,[35] and this is completely reasonable from a comparison of electrospun and cast films. In electrospinning, the polymer jet is subjected to high strains, and the velocity of fiber formation is on a millisecond scale.[37] Because of rapid solvent evaporation during electrospinning, stretched chains do not have enough time to

TABLE III
Crystallinity Degree (X_c) of PAni·TSA/PLA Blends Obtained by a Casting and Electrospinning Process

Drop-cast films			Electrospun fiber mats		
Solution	Pani·TSA (%)	X_c	Solution	PAni·TSA (%)	X_c
2	1.9	45.6	2a	1.9	29.9
			2d	1.9	38.7
3	3.8	37.2	3d	3.8	30.9
4	5.6	35.7	4a	5.6	29.3
			4b	5.6	30.1
6	1.6	57.5	6c	1.6	33.0
			6d	1.6	38.1
7	3.2	43.5	7d	3.2	24.6
8	4.7	49.9	8a	4.7	25.3
			8b	4.7	29.4
			8c	4.7	24.3
			8d	4.7	32.5

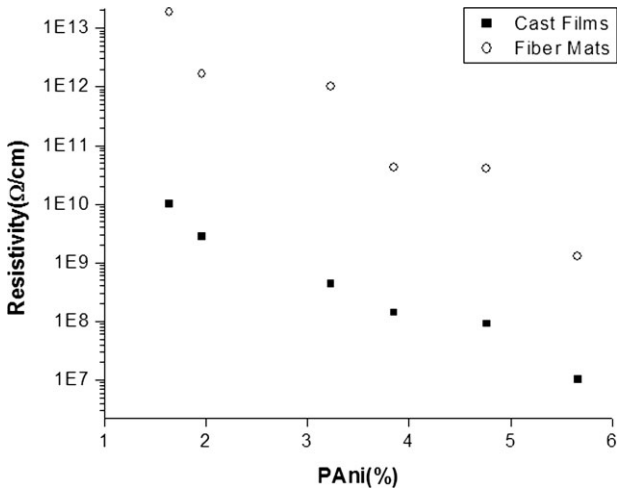

Figure 8 Effect of the PAni·TSA content on the volume resistivity of PAni·TSA/PLA blends prepared by a casting and electrospinning process.

organize into a suitable crystal structure before they solidify, and this results in lower crystallinity values.[17] In addition to the lower crystallinity values of electrospun mats, a sharp peak was observed around 5° (1.8 nm) only for mats obtained from solutions 3d and 2d, and a smaller one was observed for mats from solution 2a. These reflections can be attributed to the formation of coiled coil-like structures, as described by Hoogsteen et al.[38] Furthermore, the same samples showed minor reflections at 25 and 30°, which are related to β-crystal structures of PLA. These structures are formed under drastic strain conditions.[34] Hence, the fiber mats obtained from solutions 3d and 2d were submitted to the strongest strain conditions and, for that reason, showed the smallest average diameter values according to the results listed in Table II.

The crystallinity fractions of the polymeric samples were estimated through a comparison of the integrated intensity of the amorphous halo with the total scattered intensity with Fityk software (free peak-fitting software). Table III compares the calculated crystallinity fractions of the cast film samples with those related from electrospun fiber mats. The crystallinity of the PAni·TSA/PLA blend films decreased as the amount of PAni·TSA in the blends increased. Similar behavior was also observed for PAni·TSA/PLA fiber mats, and this indicated that the presence of PAni·TSA in the solutions disturbed the PLA crystallization, leading to low crystallinity fraction values.

The electrical resistivity of the cast films and some electrospun fibers (with average diameters in the range of 130–250 nm) is compared in Figure 8. A linear relationship between the logarithm of resistivity and the PAni concentration was obtained. The nonwoven fiber mats showed higher resistivity values than the cast films. This behavior has also been found by other authors[21] for blends of polypyrrole and poly(ethylene oxide), and it may be attributed to several factors. First, the method used for measuring the electrical conductivity might not be suitable for measuring the electrical conductivity of the nanofibers individually because of the inhomogeneity of the fiber mats as macroscopic materials. Second, the fibers are randomly distributed in the mats and present high porosity, and this makes contact between the fibers difficult. As a result, conducting pathways responsible for conductivity are hardly formed.

CONCLUSIONS

Conducting ultrafine fibers with diameters between 100 and 1000 nm were successfully produced via electrospinning from solutions of PAni·TSA/PLA blends in HFP. The smallest fiber diameters were obtained with PAni·TSA contents in the range of 2–4%. The presence of PAni in the blends significantly decreased bead formation because of changes in the dielectric constant, and this was associated with an increase in the solution viscosity and charge density. All these features contributed to higher stretching of the polymer jet during electrospinning.

Phase separations were not observed in the electrospun PAni/PLA fiber blends in this study. This indicates that the rapid evaporation of the solvent did not allow the stretched polymer chains to organize into a suitable crystal structure. The better dispersion of PAni·TSA inside the PLA matrix in the electrospun fibers and the high porosity of the nonwoven mats resulted in a decrease in the electrical conductivity in comparison with blends prepared by casting. The crystallinity of these fibers was lower than that of the corresponding blends prepared by film casting, and this could be attributed to the rapid evaporation of the solvent during the electrospinning process, which resulted in an amorphous structure rather than a crystalline structure in the fiber.

The authors are in debt to Tina Williams for the SEM analyses.

References

1. MacDiarmid, A. G.; Jones, W. E.; Norris, I. D.; Gao, J.; Johnson, A. T.; Pinto, N. J.; Hone, J.; Han, B.; Ko, F. K.; Okuzaki, H.; Laguno, M. Synth Met 2001, 199, 27.
2. Yun, M. H.; Myung, N. V.; Vasquez, R. P.; Lee, C. S.; Menke, E.; Penner, R. M. Nano Lett 2004, 4, 419.
3. Li, M.; Guo, Y.; Wei, Y.; MacDiarmid, A. G.; Lelkes, P. Y. Biomaterials 2006, 27, 2705.
4. Wnek, G. E.; Carr, M. E.; Simpson, D. G.; Bowlin, G. I. Nano Lett 2003, 3, 213.

5. Schreuder-Gibson, H.; Gibson, P.; Senecal, K.; Sennett, M.; Walker, J.; Yeomans, W.; Ziegler, D.; Tsai, P. P. Adv Mater 2002, 34, 44.
6. Gibson, P.; Gibson, H. S.; Rivin, D. Colloids Surf A 2001, 187, 469.
7. Kim, C.; Yang, K. S. Appl Phys Lett 2003, 83, 1216.
8. Choi, S. W.; Jo, S. M.; Lee, W. S.; Kim, Y. R. Adv Mater 2003, 15, 2027.
9. Liu, H.; Kameoka, J.; Czaplewski, D. A.; Craighead, H. G. Nano Lett 2004, 4, 671.
10. Aussawasathien, D.; Dong, J. H.; Dai, L. Synth Met 2005, 154, 37.
11. Manesh, K. M.; Gopalan, A. I.; Lee, K. P.; Santhosh, P.; Song, K. D.; Lee, D. D. IEEE Trans Nanotechnol 2007, 6, 513.
12. Dong, H.; Prasad, S.; Nyame, V.; Jones, W. E., Jr. Chem Mater 2004, 16, 371.
13. Ramakrishina, S.; Fujihara, K.; Teo, W. E.; Lim, T. C.; Ma, Z. An Introduction to Electrospinning and Nanofibers; World Scientific: Singapore, 2005.
14. Ko, F. K.; Aufy, A.; Lam, H.; MacDiarmid, A. G. In Wearable Electronics and Photonics; Tao, X., Ed.; CRC: Cambridge, United Kingdom, 2005; Chapter 2, p 13
15. Zeleny, J. J Phys Rev 1914, 3, 69.
16. Formhals, A. U.S. Pat. 1,975,504 (1934).
17. Zong, X.; Kim, K.; Fang, D.; Ran, S.; Hsio, B. S.; Chu, B. Polymer 2002, 43, 4403.
18. Shin, Y. M.; Hohman, M. M.; Brenner, M. P.; Rutledge, G. C. Appl Phys Lett 2001, 78, 1149.
19. Cardenas, J. R.; França, M. G. O.; Vasconcelos, E. A.; Azevedo, W. M.; Silva, E. F., Jr. J Phys D: Appl Phys 2007, 40, 1068.
20. Norris, I. D.; Shaker, M. M.; Ko, F. K.; MacDiarmid, A. G. Synth Met 2000, 114, 109.
21. Hong, K. H.; Kang, T. J. J Appl Polym Sci 2006, 99, 1277.
22. Wei, M.; Kang, B. W.; Sung, C. M.; Mead, J. Macromol Mater Eng 2006, 291, 1307.
23. Gupta, B.; Revagade, N.; Hilborn, J. Prog Polym Sci 2007, 32, 455.
24. Langer, R.; Vacanti, J. P. Tissue Eng Sci 1993, 260, 920.
25. Zong, X.; Kim, K.; Fang, D.; Ran, S.; Hsiao, B. S.; Chu, B. Polymer 2002, 43, 4403.
26. Hou, H.; Jun, Z.; Reuning, A.; Schaper, A.; Wendorff, J. H.; Greiner, A. Macromolecules 2002, 35, 2429.
27. Jun, Z.; Hou, H.; Schaper, A.; Wendorff, J. H.; Greiner, A. e-Polymers 2003, No. 009.
28. MacDiarmid, A. G.; Epstein, A. J. Faraday Discuss Chem Soc 1989, 88, 317.
29. Gu, S. Y.; Ren, J.; Vancso, G. J. Eur Polym J 2005, 41, 2559.
30. Cui, W.; Li, X.; Zhou, S.; Weng, J. J Appl Polym Sci 2007, 103, 3105.
31. Yarin, A. L. Free Liquid Jets and Films: Hydrodynamics and Rheology; Wiley: New York, 1993.
32. Fong, H.; Chun, I.; Reneker, D. H. Polymer 1999, 40, 4585.
33. Qin, X.-H.; Yang, E.-L.; Li, N.; Wang, S.-Y. J Appl Polym Sci 2007, 103, 3865.
34. Yasuniwa, M.; Sakamoto, K.; Ono, Y.; Kawahara, W. Polymer 2008, 49, 1943.
35. Zhou, H.; Green, T. B.; Joo, Y. L. Polymer 2006, 47, 7497.
36. Pouget, J. P.; Józefowicz, M. E.; Epstein, A. J.; Tang, X.; MacDiarmid, A. G. Macromolecules 1991, 24, 779.
37. Chronakis, S. I.; Grapenson, S.; Jakob, A. Polymer 2006, 47, 1597.
38. Hoogsteen, W.; Postema, A. R.; Pennings, A. J.; Brinke, G. T.; Zugenmaier, P. Macromolecules 1990, 23, 634.